Syntheses and Characterizations of Pd(II) Complexes Incorporating a *N*-Heterocyclic Carbene and Aromatic *N*-Heterocycles

Yuan Han, Han Vinh Huynh,* and Geok Kheng Tan

Department of Chemistry, National University of Singapore, 3 Science Drive 3, Singapore 117543, Singapore

Received July 25, 2007

Reaction of the bromo-bridged dimeric monocarbene complex $[PdBr_2(^iPr_2\text{-bimy})]_2$ (**1**) with various bidentate *N*-heterocycles afforded novel linear dinuclear Pd(II) complexes $\{[PdBr_2(^iPr_2\text{-bimy})]_2(\mu\text{-L})\}$-{$\mu$-L = 4,4′-bipyridine (**2**); μ-L = 4,4′-bipyridylethane (**3**); μ-L = 4,4′-bipyridylethylene (**4**)}. The mononuclear counterpart $[PdBr_2(^iPr_2\text{-bimy})(\text{pyridine})]$ (**5**) has also been synthesized by reaction of **1** with pyridine. All compounds have been fully characterized by multi-nuclei NMR spectroscopies, FAB mass spectrometry, and X-ray diffraction analyses. Molecular structures of **2**−**5** show a fixed orientation of the C−H protons in the *N*-isopropyl substituents toward the metal center, suggesting interesting C−H···Pd preagostic interactions. These interactions are retained in solution as indicated by the large downfield shift of these C−H protons in the ^{1}H NMR spectrum. UV−vis and CV studies revealed that the dinuclear complexes **2**−**4** have electrochemical behavior similar to that of the mononuclear species **5**.

Introduction

The design of regularly shaped molecules has attracted more and more interest in the last few decades.[1] Known as molecular architecture, this field is concerned with the construction of supramolecular structures by assembling metal fragments and linkers. Because of the electronic and steric versatility, aromatic *N*-heterocycles such as pyrazine and 4,4′-bipyridine have been the most widely used bridging ligands in this field.[2] In addition to their ability to connect metal centers by forming ligand−metal bonds, they provide the opportunity of π backbonding and thus may affect delocalization and transport of electrons in their complexes. A number of groups[3] have reported many macrocyclic dinuclear and polynuclear palladium complexes containing aromatic *N*-heterocycles as bridging ligands, which show promising properties in photochemistry and host−guest chemistry. It is noteworthy that in most examples the blocking ligands bound to the palladium centers are amines or phosphines. To our best knowledge, there are no existing examples containing *N*-heterocyclic carbenes (NHCs) as blocking ligands in this kind of molecule, although NHCs are currently of great interest in organometallic chemistry as a new class of ligands, due to their strong donor ability and structural versatility.[4] Recently, we have reported the synthesis and reactivity of the bromo-bridged, dimeric monocarbene complex $[PdBr_2(^iPr_2\text{-bimy})]_2$ (**1**) with the bulky *N*,*N*′-diisopropylbenzimidazolin-2-ylidene ligand ($^iPr_2$-bimy), which exhibits interesting and rare preagostic C−H···Pd interactions.[5] Herein, we report that this complex provides a convenient entry to linear dinuclear Pd(II) complexes containing bis(4-pyridyl) linkers and $^iPr_2$-bimy as supporting ligand. The resulting novel complexes can be regarded as potential building blocks toward supramolecular structures and coordination polymers.

Table 1. Comparison of Carbene Resonances and Isopropyl C−H Resonances

complex (L)	$\delta C_{carbene}$ [ppm]	δH ($\Delta\delta H$)[a] [ppm]
A (CH_3CN)	158.4[b]	6.14 (0.93)[b]
2−**5** ("Py")	158.8−159.9[d]	6.33−6.36 (1.12−1.15)[c]
B (Br^-)	165.1[c]	6.60 (1.39)[c]
C ($^iPr_2$-bimy)	180.0[c]	6.25 (1.04)[c]

[a] $\Delta\delta H = \delta H(CHMe_2$ in complex$) - \delta H(CHMe_2$ in $^iPr_2$-bimyH$^+Br^-$). [b] Measured in CD_3CN. [c] Measured in $CDCl_3$. [d] Measured in $CDCl_3$ with exception for complex **4** (in CD_2Cl_2).

Results and Discussion

Synthesis and Characterization. We recently reported that the dimeric monocarbene complex $[PdBr_2(^iPr_2\text{-bimy})]_2$ (**1**) can be readily cleaved by various monodentate ligands such as Br^-, CH_3CN, and PPh_3 to give mononuclear monocarbene species.[5] We anticipated that the extension of this cleavage reaction to

* Corresponding author. E-mail: chmhhv@nus.edu.sg.

(1) (a) Leininger, S.; Olenyuk, B.; Stang, P. J. *Chem. Rev.* **2000**, *100*, 853. (b) Swiegers, G. F.; Malefetse, T. J. *Coord. Chem. Rev.* **2002**, *225*, 91. (c) Jin, G.-X.; Arikawa, Y.; Tatsumi, K. *J. Am. Chem. Soc.* **2001**, *123*, 735. (d) Wang, J.-Q.; Ren, C.-X.; Jin, G.-X. *Chem. Commun.* **2005**, 4738. (e) Wang, J.-Q.; Ren, C.-X.; Jin, G.-X. *Organometallics* **2006**, *25*, 74. (f) Kajitani, H.; Tanabe, Y.; Kuwata, S.; Iwasaki, M.; Ishii, Y. *Organometallics* **2005**, *24*, 2251. (g) Kraft, S.; Beckhaus, R.; Haase, D.; Saak, W. *Angew. Chem., Int. Ed.* **2004**, *43*, 1583. (h) Grote, Z.; Scopelliti, R.; Severin, K. *J. Am. Chem. Soc.* **2004**, *126*, 16959.

(2) (a) Kaim, W. *Angew. Chem., Int. Ed. Engl.* **1983**, *22*, 171. (b) Kaim, W. *Coord. Chem. Rev.* **2002**, *230*, 126. (c) Berg, D. J.; Boncella, J. M.; Andersen, R. A. *Organometallics* **2002**, *21*, 4622. (d) Launay, J.-P. *Chem. Soc. Rev.* **2001**, *30*, 386. (e) Serroni, S.; Campagna, S.; Puntoriero, F.; Di Pietro, C.; McClenaghan, N.; Loiseau, F. *Chem. Soc. Rev.* **2001**, *30*, 367. (f) Kraft, S.; Hanuschek, E.; Beckhaus, R.; Haase, D.; Saak, W. *Chem.-Eur. J.* **2005**, *11*, 969.

(3) (a) Fujita, M.; Yazaki, J.; Ogura, K. *J. Am. Chem. Soc.* **1990**, *112*, 5645. (b) Fujita, M.; Yazaki, J.; Ogura, K. *Tetrahedron Lett.* **1991**, *32*, 5589. (c) Fujita, M.; Nagao, S.; Iida, M.; Ogata, K.; Ogura, K. *J. Am. Chem. Soc.* **1993**, *115*, 1574. (d) Fujita, M.; Ibukuro, F.; Yamaguchi, K.; Ogura, K. *J. Am. Chem. Soc.* **1995**, *117*, 4175. (e) Fujita, M.; Sasaki, O.; Mitsuhashi, T.; Fujita, T.; Yazaki, J.; Yamaguchi, K.; Ogura, K. *Chem. Commun.* **1996**, 1535. (f) Slone, R. V.; Yoon, D. I.; Calhoun, R. M.; Hupp, J. T. *J. Am. Chem. Soc.* **1995**, *117*, 11813. (g) Lee, S. B.; Hwang, S.; Chung, D. S.; Yun, H.; Hong, J.-I. *Tetrahedron Lett.* **1998**, *39*, 873. (h) Navarro, J. A. R.; Lippert, B. *Coord. Chem. Rev.* **2001**, *222*, 219. (i) Sun, S.-S.; Anspach, J. A.; Lees, A. J. *Inorg. Chem.* **2002**, *41*, 1862.

(4) (a) Bourissou, D.; Guerret, O.; Gabbai, F. P.; Bertrand, G. *Chem. Rev.* **2000**, *100*, 39 and references therein. (b) Hahn, F. E. *Angew. Chem., Int. Ed.* **2006**, *45*, 1348 and references therein.

(5) Huynh, H. V.; Han, Y.; Ho, J. H. H.; Tan, G. K. *Organometallics* **2006**, *25*, 3267.

10.1021/om700753d CCC: $37.00 © 2007 American Chemical Society
Publication on Web 11/02/2007

Scheme 1. Synthesis of Complexes 2−5

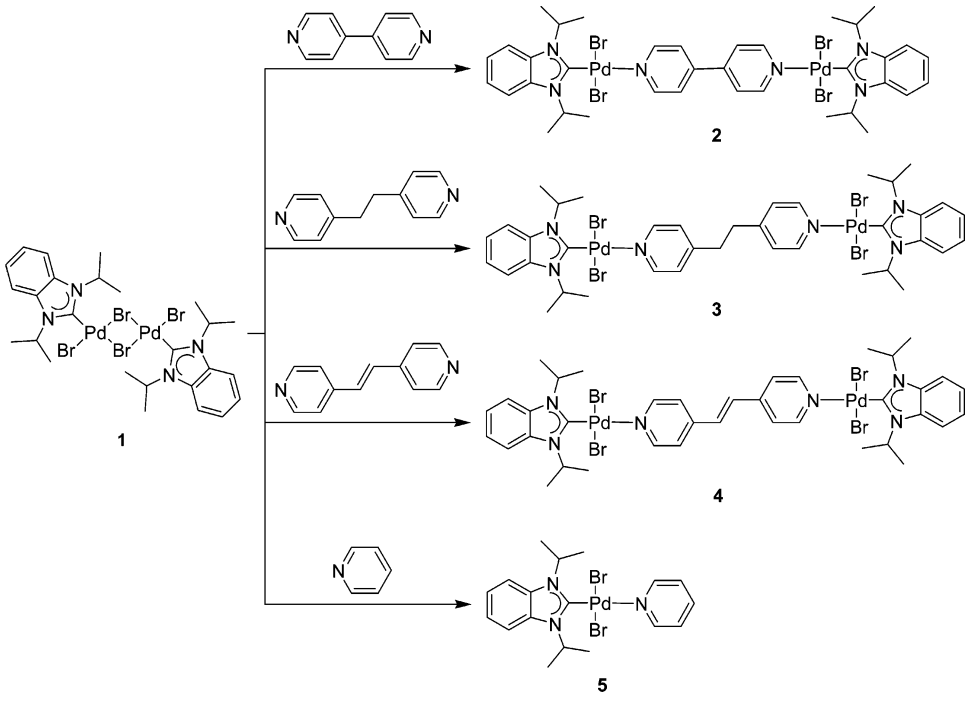

bidentate ligands should afford dinuclear Pd(II) complexes with $^{i}Pr_2$-bimy as the blocking ligand. Thus, we reacted complex **1** with a range of commercially available bis(4-pyridyl) type of ligands to test this proposal. The use of bis(4-pyridyl) ligands should give rise to highly symmetrical complexes, which in turn should ease crystallization to afford single crystals suitable for X-ray diffraction. Indeed, as shown in Scheme 1, complexes **2**−**4** were synthesized in good yields, respectively, by reacting **1** with 1 equiv of the corresponding bridging ligand in CH_2Cl_2 at room temperature. For the purpose of comparison, the mononuclear complex **5** was also prepared by stirring **1** in pyridine. The syntheses are straightforward, and all novel complexes have been isolated as yellow and air-stable solids. They are soluble in halogenated solvents, CH_3CN, DMSO, and DMF, but insoluble in nonpolar solvents such as diethyl ether, hexane, and toluene.

It is noteworthy that stoichiometry control is crucial for the efficient syntheses of the dinuclear complexes **2**−**4**. A 1:1 ratio of precursor complex **1** to the corresponding bridging ligand is important, and an excess of the latter results in a mixture of products, which can be distinguished by ^{1}H NMR spectroscopy. When complex **1** and 2 equiv of the respective bridging ligand were dissolved in CD_2Cl_2, three sets of signals were observed in the ^{1}H NMR spectrum. These signals correspond to the bridged complex, the unbridged complex, and the free ligand distinct in their 2,6-py-H resonances. The desired bridged complexes **2**−**4** show 2,6-py-H resonances, which are generally shifted downfield by 0.52−0.57 ppm as compared to those of the corresponding free ligands with the most highfield values. The unbridged complex shows two intermediate chemical shifts with the resonance for the coordinated pyridine ring being more downfield by ∼0.5 ppm as compared to that for the uncoordinated pyridine ring. The 2,6-py-H resonances of mononuclear complex **5** have values similar to those of the bridged complexes **2**−**4**. The aromatic signals and the methyl resonances of the carbene ligand remain largely unchanged upon cleavage of complex **1** and subsequent coordination of the pyridyl-based ligands, whereas the isopropyl C−H resonances are shifted highfield by ∼0.2 ppm as compared to that in the precursor complex **1**. However, these isopropyl C−H resonances appearing at 6.33−6.36 ppm in complexes **2**−**5** are still significantly more downfield than that at 5.21 ppm in the ligand precursor ($^{i}Pr_2$-bimyH$^+$Br$^-$) ($\Delta\delta H = 1.12-1.15$ ppm). This large downfield chemical shift commonly observed for Pd(II) complexes of this ligand[5,6] presumably suggests some type of interaction between the isopropyl C−H protons and the Pd center. In the literature, a few metal−hydrogen interactions (X−H···M, X = C, N) including agostic interactions,[7] preagostic interactions,[8] and hydrogen bonding[7c,9] have been described. There is no clear-cut difference between these types of interactions, but each has characteristic spectroscopic and geometric properties, which allow for a general distinction. In contrast to the upfield chemical shift of an agostic interaction and a linear X−H···M geometry of a hydrogen bond, the significant downfield chemical shift of the isopropyl C−H protons and the geometric parameters (vide infra) observed for complexes **2**−**5** best fit the definition of a preagostic interaction. Such an interaction has recently been observed in Rh(I) complexes of NHC ligands as well.[10] Although the origin of such interactions is still under debate,[7c,8c−e]

(6) Han, Y.; Huynh, H. V.; Koh, L. L. *J. Organomet. Chem.* **2007**, *692*, 3606.

(7) (a) Brookhart, M.; Green, M. L. H. *J. Organomet. Chem.* **1983**, *250*, 395. (b) Crabtree, R. H. *Angew. Chem., Int. Ed. Engl.* **1993**, *32*, 789. (c) Yao, W.; Eisenstein, O.; Crabtree, R. H. *Inorg. Chim. Acta* **1997**, *254*, 105.

(8) (a) Bortolin, M.; Bucher, U.; Reugger, H.; Venanzi, L. M.; Albinati, A.; Lianza, F. *Organometallics* **1992**, *11*, 2514. (b) Cano, M.; Heras, J. V.; Maeso, M.; Alvaro, M.; Fernández, R.; Pinilla, E.; Campo, J. A.; Monge, A. *J. Organomet. Chem.* **1997**, *534*, 159. (c) Zhang, Y.; Lewis, J. C.; Bergman, R. G.; Ellman, J. A.; Oldfield, E. *Organometallics* **2006**, *25*, 3515. (d) Lewis, J. C.; Wu, J.; Bergman, R. G.; Ellman, J. *Organometallics* **2005**, *24*, 5737. (e) Brammer, L. *Dalton Trans.* **2003**, 3145.

(9) (a) Brammer, L.; Charnock, J. M.; Goggin, P. L.; Goodfellow, R. J.; Koetzle, T. F.; Orpen, A. J. *J. Chem. Soc., Chem. Commun.* **1987**, 443. (b) Lee, J. C.; Rheingold, A. L.; Muller, B.; Pregosin, P. S.; Crabtree, R. H. *J. Chem. Soc., Chem. Commun.* **1994**, 1021. (c) Brammer, L.; McCann, M. C.; Bullock, R. M.; McMullan, R. K.; Sherwood, P. *Organometallics* **1992**, *11*, 2339. (d) Braga, D.; Grepioni, F.; Tedesco, E. *Organometallics* **1997**, *16*, 1846.

(10) (a) Bazinet, P.; Yap, G. P. A.; Richeson, D. S. *J. Am. Chem. Soc.* **2003**, *125*, 13314. (b) Gómez-Bujedo, S.; Alcarazo, M.; Pichon, C.; Álvarez, E.; Fernández, R.; Lassaletta, J. M. *Chem. Commun.* **2007**, 1180.

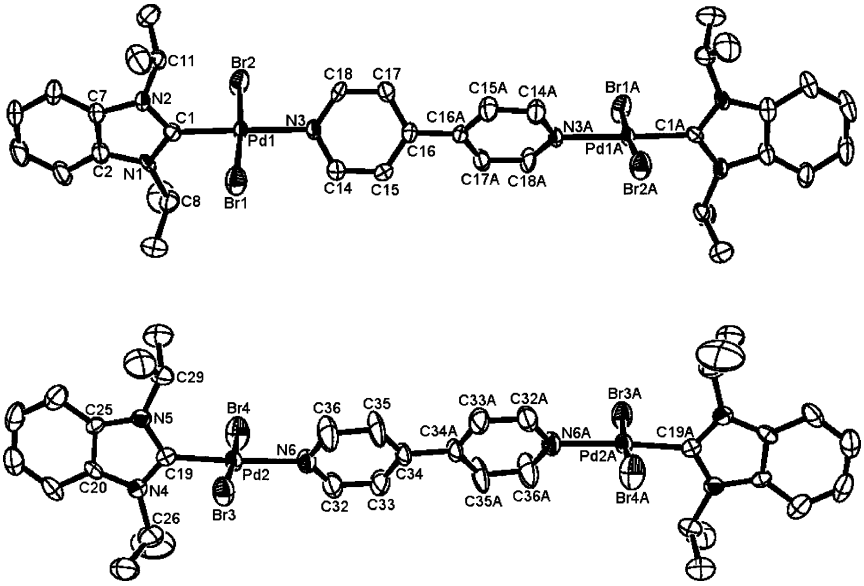

Figure 1. Molecular structures of the two independent molecules in the solid state of complex **2**·2THF showing 50% probability ellipsoids: (a) with the two twisted pyridine rings (top); (b) with the two coplanar pyridine rings (bottom); hydrogen atoms and solvent molecules are omitted for clarity.

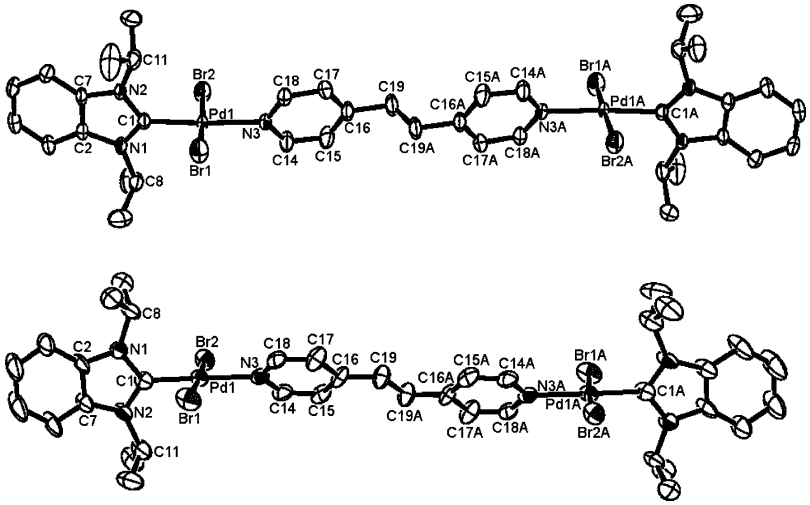

Figure 2. Molecular structures of complex **3** (top) and complex **4**·4CH_2Cl_2 (bottom) showing 50% probability ellipsoids; hydrogen atoms and solvent molecules are omitted for clarity.

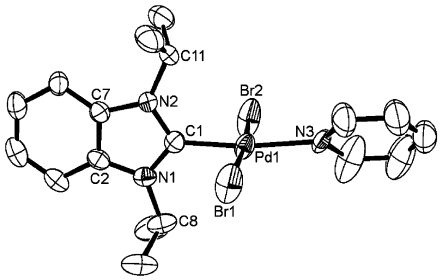

Figure 3. Molecular structure of complex **5** showing 50% probability ellipsoids; hydrogen atoms and one of the two disordered pyridine rings are omitted for clarity.

DFT calculations have indicated the involvement of filled $d_{xz/yz}$ metal orbitals.[8c]

Furthermore, the ^{13}C NMR spectra of complexes **2**−**5** show the carbene carbon resonances in a narrow range of 158.8−159.9 ppm. Herrmann and more recently Baker[11] found that the ^{13}C NMR chemical shift of the carbene carbon decreases as the Lewis acidity of the metal center increases. Obviously, this is directly related to the σ-donor ability of the co-ligands. This hypothesis is remarkably well corroborated when the carbene resonances of the previously reported complexes *trans*-$[PdBr_2(^iPr_2\text{-bimy})L]^{n-}$ {L = CH_3CN, $n = 0$ (**A**);[5] L = Br^-, $n = 1$ (**B**),[5] L = $^iPr_2$-bimy, $n = 0$ (**C**)[6]} are compared to those of complexes **2**−**5** (Table 1). In this series, the weakest σ-donor, CH_3CN, leads to the most upfield, whereas coordination of the strongest σ-donor, $^iPr_2$-bimy, results in the most downfield ^{13}C chemical shift. In between, the bromo ligand is found to be a stronger σ-donor than pyridyl-based ligands. Interestingly, the same trend is also observed for the isopropyl C−H resonances of the carbene ligand with the exception of complex **C** (Table 1). Apparently, an increase in the Lewis acidity of the metal center leads to a weaker preagostic interaction, which in turn results in a smaller downfield shift.[7c,8c] The deviation of complex **C** from this trend is most likely due to the competition of 4 as compared to only 2 C−H protons for the electron density of the filled $d_{xz/yz}$ metal orbital. Moreover, the ^{13}C chemical shift

(11) (a) Herrmann, W. A.; Runte, O.; Artus, G. *J. Organomet. Chem.* **1995**, *501*, C1. (b) Baker, M. V.; Barnard, P. J.; Brayshaw, S. K.; Hickey, J. L.; Skelton, B. W.; White, A. H. *Dalton Trans.* **2005**, 37.

Table 2. Selected Bond Lengths [Å] and Angles [deg] for Complexes 2−5

				2·2THF		
	3	**4**·4CH_2Cl_2	**5**	molecule a	molecule b	
Pd1−C1	1.956(3)	1.943(10)	1.953(4)	1.959(7)	Pd2−C19	1.955(8)
Pd1−Br1	2.4250(4)	2.4167(14)	2.4113(7)	2.4238(11)	Pd2−Br3	2.4313(12)
Pd1−Br2	2.4254(4)	2.4234(14)	2.4310(6)	2.4293(12)	Pd2−Br4	2.4304(12)
Pd1−N3	2.094(2)	2.112(8)	2.113(3), 2.154(3)[a]	2.102(6)	Pd2−N6	2.101(7)
N1−C1	1.344(3)	1.363(11)	1.352(5)	1.346(9)	N4−C19	1.336(10)
N1−C2	1.400(3)	1.410(12)	1.391(5)	1.402(9)	N4−C20	1.392(10)
N1−C8	1.467(4)	1.464(12)	1.474(5)	1.483(10)	N4−C26	1.470(12)
N2−C1	1.349(3)	1.354(12)	1.342(5)	1.321(9)	N5−C19	1.341(10)
N2−C7	1.401(3)	1.385(13)	1.400(5)	1.404(10)	N5−C25	1.395(10)
N2−C11	1.484(3)	1.494(12)	1.474(5)	1.482(10)	N5−C29	1.476(10)
C2−C7	1.388(4)	1.387(13)	1.379(5)	1.389(12)	C20−C25	1.388(11)
N3−C14	1.328(4)	1.337(11)	1.3900	1.351(10)	N6−C32	1.303(12)
N3−C18	1.340(4)	1.331(11)	1.3900	1.317(11)	N6−C36	1.299(13)
C14−C15	1.379(4)	1.361(13)	1.3900	1.378(11)	C32−C33	1.386(13)
C15−C16	1.391(4)	1.406(12)	1.3900	1.372(11)	C33−C34	1.361(14)
C16−C17	1.373(4)	1.387(14)	1.3900	1.373(11)	C34−C35	1.346(13)
C17−C18	1.378(4)	1.354(13)	1.3900	1.369(11)	C35−C36	1.401(13)
C16−C19	1.513(4)	1.451(13)				
C19−C19A	1.520(6)	1.357(18)				
C16−C16A				1.477(13)	C34−C34A	1.490(15)
C1−Pd1−Br1	91.59(8)	88.7(3)	86.77(10)	88.0(2)	C19−Pd2−Br3	89.0(2)
C1−Pd1−Br2	85.85(8)	86.7(3)	86.63(10)	88.3(2)	C19−Pd2−Br4	86.8(2)
N3−Pd1−Br1	92.05(7)	92.7(2)	91.23(12), 96.13(12)[a]	92.2(2)	N6−Pd2−Br3	92.8(2)
N3−Pd1−Br2	90.36(7)	91.8(2)	95.83(12), 90.29(12)[a]	91.6(2)	N6−Pd2−Br4	91.4(2)
C1−N1−C2	110.0(2)	108.4(8)	109.6(3)	108.8(6)	C19−N4−C20	109.1(7)
C1−N2−C7	110.0(2)	109.3(8)	109.4(3)	109.7(7)	C19−N5−C25	109.9(6)
N1−C1−N2	107.5(2)	108.3(8)	107.7(3)	109.1(6)	N4−C19−N5	108.4(7)
C14−N3−C18	117.4(3)	118.1(8)	120.0	117.6(7)	C32−N6−C36	116.7(8)
$PdCNBr_2$/carbene dihedral angle	80.98	88.99	85.11, 85.08[a]	88.25		89.32
$PdCNBr_2$/pyridine ring dihedral angle	66.38	46.26	47.95, 26.01[a]	58.90		63.24

[a] Data for complex **5** with the other disordered pyridine ring.

of the carbene atom in complex **5** is more downfield by 9.8 ppm than that found in the platinum analogue *trans*-[$PtBr_2$(^{i}-Pr_2-bimy)(pyridine)].[12] Similar downfield shifts of the carbene resonances upon replacement of Pt by Pd have been reported by others.[13]

Finally, the formation of complexes **2**−**5** was further supported by their positive mode FAB mass spectra, which show the fragment peaks $[M - Br]^+$ arising from loss of one bromo ligand.

Molecular Structures. Single crystals of **2**−**5** suitable for X-ray diffraction analysis were obtained from a THF solution (**2**) or from dichloromethane/diethyl ether solutions (**3**−**5**). Their molecular structures are depicted in Figures 1−3, selected bond parameters are summarized in Table 2, and crystallographic data are listed in Table 3. Complex **2** crystallizes as THF solvate **2**·2THF with an unusually long axis of $c = 64.853(3)$ Å. Two independent molecules can be found, which are readily distinguished by the twisted (**2a**, torsion angle 46.22°, Figure 1, top) or coplanar arrangements of the two pyridine rings (**2b**, Figure 1, bottom). The structure of solvate **4**·4CH_2Cl_2 (Figure 2, bottom) illustrates a trans configuration across the double bond of 4,4′-bipyridylethylene, which results in the linear geometry of the complex. The molecular structure of complex **5** shows disorder of the pyridine ring into two positions with the occupancy ratio of 50:50. For clarity purpose, only one of the disordered pyridine rings is shown in Figure 3. All four complexes crystallized as trans configured complexes, in which each palladium center is surrounded by one carbene, one pyridyl-based ligand, and two bromo ligands in a nearly perfect square planar fashion. The carbene ring planes of all complexes are oriented almost perpendicularly to the $PdCNBr_2$ coordination plane with dihedral angles ranging from 80.98° to 89.32°, which are typical for NHC complexes to relieve steric congestion. On the other hand, the pyridine ring planes deviate from the perpendicular orientation with respect to the $PdCNBr_2$ coordination plane in torsion angles of 58.90° for **2a**, 63.24° for **2b**, 66.38° for **3**, 46.26° for **4**, and 47.95° and 26.01° for **5**. Furthermore, there are no indications of intermolecular $\pi-\pi$ interactions in the solid state. The Pd−$C_{carbene}$ bonds that amount to 1.943−1.959 Å in complexes **2**−**5** are close to that found in the precursor complex **1** (1.947(3) Å). The Pd−N bonds fall in a narrow range of 2.094(2)−2.154(3) Å and are comparable to those found in the commercially available and remarkably active PEPPSI catalyst[14] representing an imidazolin-2-ylidene analogue of complex **5**. More importantly, all C−H protons of the isopropyl groups are oriented toward the metal center resulting in relatively short C−H···Pd distances. These structural proper-

(12) Han, Y.; Huynh, H. V.; Tan, G. K. *Organometallics* **2007**, *26*, 4612.

(13) (a) Cardin, D. J.; Cetinkaya, B.; Cetinkaya, E.; Lappert, M. F.; Randall, E. W.; Rosenberg, E. *J. Chem. Soc., Dalton Trans.* **1973**, 1982. (b) Hiraki, K.; Onishi, M.; Ohnuma, K.; Sugino, K. *J. Organomet. Chem.* **1981**, *216*, 413. (c) Ku, R.-Z.; Huang, J.-C.; Cho, J.-Y.; Kiang, F.-M.; Reddy, K. R.; Chen, Y.-C.; Lee, K.-J.; Lee, J.-H.; Lee, G.-H.; Peng, S.-M.; Liu, S.-T. *Organometallics* **1999**, *18*, 2145.

(14) (a) O'Brien, C. J.; Kantchev, E. A. B.; Valente, C.; Hadei, N.; Chass, G. A.; Lough, A.; Hopkinson, A. C.; Organ, M. G. *Chem.-Eur. J.* **2006**, *12*, 4743. (b) Kantchev, E. A. B.; O'Brien, C. J.; Organ, M. G. *Aldrichimica Acta* **2006**, *39*, 97.

Table 3. Selected Crystallographic Data for Complexes 2−5

	2·2THF	**3**	**4**·4CH_2Cl_2	**5**
formula	$C_{44}H_{60}Br_4N_6O_2Pd_2$	$C_{38}H_{48}Br_4N_6Pd_2$	$C_{42}H_{54}Br_4Cl_8N_6Pd_2$	$C_{18}H_{23}Br_2N_3Pd$
formula weight	1237.42	1121.26	1458.95	547.61
color, habit	orange, block	yellow, block	yellow, needle	colorless, block
crystal size [mm]	0.56 × 0.54 × 0.14	0.36 × 0.30 × 0.10	0.56 × 0.09 × 0.08	0.40 × 0.36 × 0.08
temp [K]	223(2)	223(2)	223(2)	223(2)
crystal system	monoclinic	monoclinic	monoclinic	orthorhombic
space group	*C*2/*c*	*P*2(1)/*c*	*P*2(1)/*n*	*Iba*2
a [Å]	14.9471(7)	14.9211(8)	13.348(6)	16.990(4)
b [Å]	10.1197(4)	9.9826(6)	9.175(4)	24.792(6)
c [Å]	64.853(3)	16.1261(9)	22.350(10)	9.693(2)
α [deg]	90	90	90	90
β [deg]	90.1380(10)	116.7250(10)	102.540(10)	90
γ [deg]	90	90	90	90
V [Å^3]	9809.6(7)	2145.4(2)	2672(2)	4083.0(16)
Z	8	2	2	8
D_c [g cm^{-3}]	1.676	1.736	1.813	1.782
radiation used	Mo Kα	Mo Kα	Mo Kα	Mo Kα
μ [mm^{-1}]	4.032	4.596	4.100	4.828
θ range [deg]	1.88−27.50	1.53−27.48	1.64−25.00	1.45−27.49
unique data	32 683	14 640	15 058	25 995
max, min transmission	0.6021, 0.2111	0.6564, 0.2884	0.7350, 0.2073	0.6987, 0.2483
final *R* indices [$I > 2\sigma(I)$]	R1 = 0.0788, wR2 = 0.1699	R1 = 0.0312, wR2 = 0.0688	R1 = 0.0643, wR2 = 0.1593	R1 = 0.0298, wR2 = 0.0730
R indices (all data)	R1 = 0.0960, wR2 = 0.1762	R1 = 0.0432, wR2 = 0.0731	R1 = 0.1155, wR2 = 0.1805	R1 = 0.0346, wR2 = 0.0756
GOF on F^2	1.184	1.018	1.022	1.033
peak/hole [e Å^{-3}]	1.480/−1.271	0.596/−0.477	0.983/−0.896	0.750/−0.411

Table 4. Comparison of Selected Structural and Spectroscopic Data for Complexes 2−5

complex	*d*(C−H···Pd) [Å]	*θ*(C−H···Pd) [deg]	*δH* (Δ*δH*)[a] [ppm]
2	2.667, 2.706[d]	121.23, 121.27	6.33 (1.12)[b]
	2.649, 2.770[e]	121.27, 121.41	
3	2.725, 2.758	119.81, 119.87	6.33 (1.12)[b]
4	2.707, 2.731	120.42, 120.02	6.36 (1.15)[c]
5	2.654, 2.751	119.91, 121.33	6.34 (1.13)[b]

[a] $\Delta\delta H = \delta H$(C*H*Me$_2$ in complex) − δH(C*H*Me$_2$ in ^{i}Pr$_2$-bimyH$^+$Br$^-$). [b] Measured in $CDCl_3$. [c] Measured in CD_2Cl_2. [d] For molecule a. [e] For molecule b.

Table 5. UV−Vis Absorption Spectral Data of Complexes 1−5 in CH_2Cl_2 at Room Temperature

complex	λ_{max}, nm ($10^{-3}\epsilon$, M^{-1} cm^{-1})
1	242 (sh, 45.1), 276 (28.5), 282 (28.0)
2	241 (sh, 54.5), 277 (45.7), 283 (46.6), 360 (1.18)
3	231 (sh, 66.4), 276 (sh, 32.2), 282 (31.8), 359 (1.40)
4	231 (sh, 52.2), 283 (sh, 43.7), 307 (57.7), 317 (56.9)
5	239 (sh, 25.6), 276 (sh, 14.1), 282 (13.9), 367 (0.50)

ties support the aforementioned C−H···Pd preagostic interactions as indicated by ^{1}H NMR spectroscopy. A comparison of structural and spectroscopic data supporting these interactions for all complexes discussed here is shown in Table 4.

Electronic Properties of the Complexes. The UV−vis absorption spectral data obtained for complexes **2**−**5** and their precursor complex **1** in CH_2Cl_2 are summarized in Table 5. Complexes **2**, **3**, and **5** show very weak absorption bands at 355−370 nm corresponding to the metal-to-ligand charge-transfer (MLCT).[15] Furthermore, the spectra of complexes **1**, **2**, and **5** exhibited absorbance maxima at ca. 240, 275, and 280 nm, which are assigned to intraligand $\pi\rightarrow\pi^*$ transitions. However, for complexes **3** and **4**, the highest energy transitions are blue-shifted and centered at ca. 230 nm. Complex **4** also shows two intense red-shifted bands at 306 and 317 nm probably due to the additional double bond in the bridging ligand, which results in an extended conjugation. No luminescence was observed from any of these complexes at ambient temperature in CH_2Cl_2 solutions.

Cyclic voltammograms (CV) of complexes **2**−**5** were recorded in CH_3CN. The dinuclear complexes **2**−**4** behave rather similarly to the mononuclear complex **5**. All CVs are nearly identical, and each exhibits only an irreversible reduction wave at about −1375 mV versus $[Cp_2Fe]^0/[Cp_2Fe]^+$, possibly corresponding to the reduction of Pd(II) to Pd(0) species and subsequent decomposition. The fact that only one reduction wave was observed for each of the dinuclear species leads to the assumption that no strong intramolecular communication of the Pd centers exists in these complexes.

Conclusion

A series of linear dinuclear Pd(II) complexes **2**−**4** containing bis(4-pyridyl) linkers and the bulky ^{i}Pr-bimy as the supporting ligand have been prepared by reacting the dimeric monocarbene complex **1** with the respective bridging ligand. Their mononuclear counterpart **5** was also synthesized. The molecular structures of all complexes show a fixed orientation of the *N*-isopropyl substituents with the C−H protons pointing to the metal center to maximize interesting and rare C−H···Pd preagostic interactions. The large downfield shift of these protons in the ^{1}H NMR spectrum indicates that these interactions are retained in solution. UV−vis and CV analyses revealed that the electrochemical behavior of the dinuclear complexes **2**−**4** is similar to that of the mononuclear species **5**. Further studies are underway to explore the potential of these dinuclear complexes as building blocks toward supramolecular structures and coordination polymers.

Experimental Section

General Considerations. Unless otherwise noted, all operations were performed without taking precautions to exclude air and moisture, and all chemicals and solvents were used as received without any further treatment. Complex **1** was prepared as previ-

(15) Wolf, P. de; Heath, S. L.; Thomas, J. A. *Chem. Commun.* **2002**, 2540.

ously reported.[5] ^{1}H and ^{13}C NMR spectra were recorded on a Bruker ACF 300 spectrometer, and the chemical shifts (δ) were internally referenced by the residual solvent signals relative to tetramethylsilane. Mass spectra were measured using a Finnigan MAT LCQ (FAB) spectrometer. Elemental analyses were performed on a Perkin-Elmer PE 2400 elemental analyzer at the Department of Chemistry, National University of Singapore. Cyclic voltammograms were measured on an ECO/Metrohm, PGSTAT 30 potentiostat/galvanostat, and UV/vis spectra were obtained using a Hewlett-Packard HP8452A diode array spectrophotometer.

4,4′-Bipyridine-Bridged Complex (2). A mixture of complex **1** (94 mg, 0.10 mmol) and 4,4′-bipyridine (16 mg, 0.10 mmol) was dissolved in CH_2Cl_2 (5 mL) and stirred at ambient temperature overnight. The reaction mixture was filtered over Celite. Slow evaporation of CH_2Cl_2 afforded the product as yellow crystals (93 mg, 0.085 mmol, 85%). ^{1}H NMR (300 MHz, $CDCl_3$): δ 9.32 (d, ^3J(H,H) = 6.7 Hz, 4H, 2,6-bpy-H), 7.61−7.58 (m, 8H, 3,5-bpy-H and Ar−H), 7.24 (dd, 4H, Ar−H), 6.33 (m, ^3J(H,H) = 7.1 Hz, 4H, NC*H*$(CH_3)_2$), 1.81 (d, ^3J(H,H) = 7.1 Hz, 24H, CH_3). ^{13}C{^{1}H} NMR (75.47 MHz, $CDCl_3$): 158.8 (s, NCN), 153.8, 146.3, 133.7, 122.5, 122.4, 112.8 (s, bpy−C and Ar−C), 54.8 (s, N*C*H$(CH_3)_2$), 20.8 (s, CH_3). Anal. Calcd for $C_{36}H_{44}N_6Br_4Pd_2$: C, 39.55; H, 4.06; N, 7.69. Found: C, 39.94; H, 4.56; N, 7.36. MS (FAB): m/z = 1013 $[M - Br]^+$.

4,4′-Bipyridylethane-Bridged Complex (3). Complex **3** was prepared in analogy to **2** from complex **1** (94 mg, 0.10 mmol) and 4,4′-bipyridylethane (18 mg, 0.10 mmol). Crystallization from a dichloromethane/diethyl ether mixture afforded the product as yellow crystals (99 mg, 0.088 mmol, 88%). ^{1}H NMR (300 MHz, $CDCl_3$): δ 9.04 (d, ^3J(H,H) = 6.6 Hz, 4H, 2,6-py-H), 7.59 (dd, 4H, Ar−H), 7.22 (dd, 4H, Ar−H), 7.18 (d, ^3J(H,H) = 6.6 Hz, 4H, 3,5-py-H), 6.33 (m, ^3J(H,H) = 7.1 Hz, 4H, NC*H*$(CH_3)_2$), 2.95 (s, 4H, CH_2), 1.79 (d, ^3J(H,H) = 7.1 Hz, 24H, CH_3). ^{13}C{^{1}H} NMR (75.47 MHz, $CDCl_3$): 159.5 (s, NCN), 152.8, 151.7, 133.6, 124.5, 122.4, 112.7 (s, py−C and Ar−C), 54.7 (s, N*C*H$(CH_3)_2$), 35.4 (s, CH_2), 20.7 (s, CH_3). Anal. Calcd for $C_{38}H_{48}Br_4N_6Pd_2$: C, 40.70; H, 4.31; N, 7.49. Found: C, 40.60; H, 4.44; N, 7.40. MS (FAB): m/z = 1041 $[M - Br]^+$.

4,4′-Bipyridylethylene-Bridged Complex (4). Complex **4** was prepared in analogy to **2** from complex **1** (94 mg, 0.10 mmol) and 4,4′-bipyridylethylene (18 mg, 0.10 mmol). Slow evaporation at ambient temperature of a concentrated CH_2Cl_2 solution afforded the product as yellow crystals (106 mg, 0.095 mmol, 95%). ^{1}H NMR (300 MHz, CD_2Cl_2): δ 9.16 (d, ^3J(H,H) = 6.7 Hz, 4H, 2,6-py-H), 7.66 (dd, 4H, Ar−H), 7.56 (d, ^3J(H,H) = 6.7 Hz, 4H, 3,5-py-H), 7.37 (s, 2H, CH═CH), 7.29 (dd, 4H, Ar−H), 6.36 (m, ^3J(H,H) = 7.1 Hz, 4H, NC*H*$(CH_3)_2$), 1.82 (d, ^3J(H,H) = 7.1 Hz, 24H, CH_3). ^{13}C{^{1}H} NMR (75.47 MHz, CD_2Cl_2): 159.6 (s, NCN), 152.8, 144.9, 133.3 (s, py−C and Ar−C), 131.2 (s, CH═CH), 122.2, 121.9, 112.5 (s, py−C and Ar−C), 54.5 (s, N*C*H$(CH_3)_2$), 20.2 (s, CH_3). Anal. Calcd for $C_{38}H_{46}Br_4N_6Pd_2$: C, 40.78; H, 4.14; N, 7.51. Found: C, 41.09; H, 3.91; N, 7.53. MS (FAB): m/z = 1039 $[M - Br]^+$.

***trans*-Dibromo(1,3-diisopropylbenzimidazolin-2-ylidene)(pyridine)palladium(II) (5).** Complex **1** (47 mg, 0.05 mmol) was dissolved in pyridine (3 mL) and stirred at ambient temperature overnight. The reaction mixture was filtered over Celite. The Celite was repeatedly washed with CH_2Cl_2 until it was white. All volatiles of the filtrate were removed in vacuo to give the product as a yellow powder (45 mg, 0.082 mmol, 82%). ^{1}H NMR (300 MHz, $CDCl_3$): δ 9.13 (m, 2H, 2,6-py-H), 7.78 (m, 1H, 4-py-H), 7.59 (dd, 2H, Ar−H), 7.36 (m, 2H, 3,5-py-H), 7.22 (dd, 2H, Ar−H), 6.34 (m, ^3J(H,H) = 7.1 Hz, 2H, NC*H*$(CH_3)_2$), 1.79 (d, ^3J(H,H) = 7.1 Hz, 12H, CH_3). ^{13}C{^{1}H} NMR (75.47 MHz, $CDCl_3$): 159.5 (s, NCN), 152.9, 138.0, 133.6, 124.7, 122.4, 112.8 (s, Ar−C), 54.7 (s, N*C*H$(CH_3)_2$), 20.7 (s, CH_3). Anal. Calcd for $C_{18}H_{23}N_3Br_2Pd$: C, 39.48; H, 4.23; N, 7.67. Found: C, 39.50; H, 4.11; N, 7.55. MS (FAB): m/z = 468 $[M - Br]^+$.

X-ray Diffraction Studies. Diffraction data for complexes **2**−**5** were collected with a Bruker AXS APEX CCD diffractometer equipped with a rotation anode at 223(2) K using graphite monochromated Mo Kα radiation (λ = 0.71073 Å). Data were collected over the full sphere and were corrected for absorption. Structure solutions were found by the Patterson method. Structure refinement was carried out by full-matrix least-squares on F^2 using SHELXL-97[16] with first isotropic and later anisotropic displacement parameters for all non-hydrogen atoms. A summary of the most important crystallographic data is given in Table 3.

Acknowledgment. We thank the National University of Singapore for financial support (Grant No. R 143-000-268-112) and acknowledge the technical assistance from our department. We are also grateful to Dr. Wolfram W. Seidel and Matthias Meel for the CV measurements.

Supporting Information Available: Crystallographic data for **2**−**5** as CIF files. This material is available free of charge via the Internet at http://pubs.acs.org.

OM700753D

(16) Sheldrick, G. M. *SHELXL-97*; Universität Göttingen: Germany, 1997.